

# Insulin-Mediated Acceleration of Breast Cancer Development and Progression in a Nonobese Model of Type 2 Diabetes

Ruslan Novosyadlyy<sup>1</sup>, Danielle E. Lann<sup>1</sup>, Archana Vijayakumar<sup>1</sup>, Anne Rowzee<sup>2</sup>, Deborah A. Lazzarino<sup>2</sup>, Yvonne Fierz<sup>1</sup>, Joan M. Carboni<sup>3</sup>, Marco M. Gottardis<sup>3</sup>, Patricia A. Pennisi<sup>4</sup>, Alfredo A. Molinolo<sup>5</sup>, Naamit Kurshan<sup>1</sup>, Wilson Mejia<sup>1</sup>, Stefania Santopietro<sup>4</sup>, Shoshana Yakar<sup>1</sup>, Teresa L. Wood<sup>2</sup>, and Derek LeRoith<sup>1</sup>

## Abstract

Epidemiologic studies suggest that type 2 diabetes (T2D) increases breast cancer risk and mortality, but there is limited experimental evidence supporting this association. Moreover, there has not been any definition of a pathophysiological pathway that diabetes may use to promote tumorigenesis. In the present study, we used the MKR mouse model of T2D to investigate molecular mechanisms that link T2D to breast cancer development and progression. MKR mice harbor a transgene encoding a dominant-negative, kinase-dead human insulin-like growth factor-I receptor (IGF-IR) that is expressed exclusively in skeletal muscle, where it acts to inactivate endogenous insulin receptor (IR) and IGF-IR. Although lean female MKR mice are insulin resistant and glucose intolerant, displaying accelerated mammary gland development and enhanced phosphorylation of IR/IGF-IR and Akt in mammary tissue, in the context of three different mouse models of breast cancer, these metabolic abnormalities were found to accelerate the development of hyperplastic precancerous lesions. Normal or malignant mammary tissue isolated from these mice exhibited increased phosphorylation of IR/IGF-IR and Akt, whereas extracellular signal-regulated kinase 1/2 phosphorylation was largely unaffected. Tumor-promoting effects of T2D in the models were reversed by pharmacological blockade of IR/IGF-IR signaling by the small-molecule tyrosine kinase inhibitor BMS-536924. Our findings offer compelling experimental evidence that T2D accelerates mammary gland development and carcinogenesis, and that the IR and/or the IGF-IR are major mediators of these effects. *Cancer Res*; 70(2): 741–51. ©2010 AACR.

## Introduction

Epidemiologic studies suggest that obesity and type 2 diabetes (T2D) significantly increase overall cancer risk and mortality. One of the malignancies adversely affected by obesity and T2D is breast cancer (1–5), the second most common cancer in the world, which will be diagnosed in 25 million women over the next 25 years.

Numerous factors can potentially be implicated in the tumor-promoting activity of obesity, including increased influx of nutrients, elevated circulating insulin-like growth factor-I (IGF-I) levels, and enhanced secretion of adipokines, proinflammatory cytokines, sex steroids, and growth factors by adipose tissue (6–8). However, epidemiologic data indicate that

T2D exerts tumor-promoting activity independent of obesity (4, 9). This effect of T2D is thought to be mediated by the characteristic hallmarks of the disease: hyperinsulinemia, hyperglycemia, and/or hyperlipidemia (10).

Animal studies investigating the relationship between obesity, diabetes, and breast cancer provide scarce and inconclusive results. Most of them confirm a stimulatory effect of obesity on breast cancer development (11), but they do not differentiate between obesity- and diabetes-related effects and fail to identify pathophysiologic mechanisms implicated in the tumor-promoting activity.

In the current work, we provide novel experimental evidence that diabetes-related hyperinsulinemia affects mammary gland development and breast cancer progression independent of

**Authors' Affiliations:** <sup>1</sup>Division of Endocrinology, Diabetes and Bone Diseases, The Samuel Bronfman Department of Medicine, Mount Sinai School of Medicine, New York, New York; <sup>2</sup>Department of Neurology and Neurosciences, New Jersey Medical School, University of Medicine and Dentistry of New Jersey, Newark, New Jersey; <sup>3</sup>Oncology Drug Discovery, Bristol Myers Squibb Research Institute, Princeton, New Jersey; and <sup>4</sup>Diabetes Branch, National Institute of Diabetes, Digestive and Kidney Diseases and <sup>5</sup>National Institute of Dental and Craniofacial Research, NIH, Bethesda, Maryland

**Note:** Supplementary data for this article are available at Cancer Research Online (<http://cancerres.aacrjournals.org/>).

R. Novosyadlyy and D.E. Lann contributed equally to this work.

Current address for A. Rowzee: National Institute of Dental and

Craniofacial Research, NIH, Bethesda, MD; current address for P.A. Pennisi: Centro de Investigaciones Endocrinológicas (CEDIE-CONICET), Hospital de Niños "Dr. Ricardo Gutiérrez Gallo," Buenos Aires, Argentina; current address for W. Mejia: Department of Nutrition and Biochemistry, Pontificia Universidad Javeriana, Bogota, Colombia; current address for S. Santopietro: National Cancer Institute, NIH, Bethesda, MD.

**Corresponding Author:** Derek LeRoith, Division of Endocrinology, Diabetes and Bone Diseases, The Samuel Bronfman Department of Medicine, Mount Sinai School of Medicine, New York, NY 10029. Phone: 212-241-7429; Fax: 212-241-4218; E-mail: derek.leroith@mssm.edu.

doi: 10.1158/0008-5472.CAN-09-2141

©2010 American Association for Cancer Research.

obesity. Hyperinsulinemia mediates these effects by activating the insulin receptor (IR), the IGF-I receptor (IGF-IR), and the phosphoinositide 3-kinase (PI3K) pathway.

Given the pandemic of obesity and T2D, this study will have a significant effect on public health and patient outcomes worldwide. It will help to develop preventative and therapeutic options, whereby breast cancer morbidity and mortality may eventually be reduced. The results of this work can be quickly translated into clinical practice that will help to optimize adjuvant and neoadjuvant therapy in breast cancer patients with T2D.

## Materials and Methods

**Animals.** All animals were housed and maintained in an animal facility at the Mount Sinai School of Medicine. Mice were kept on a 12-h light/dark cycle with access to a standard laboratory chow diet and fresh water *ad libitum*. Generation of MMTV-PyVMT and MKR transgenic mice was described previously (12, 13). MMTV-PyVMT mice were kindly donated by W.J. Muller (McGill University, Montreal, Quebec, Canada).

**PyVMT/MKR transgenic tumor model.** All the mice used in this study were on the FVB/N background. PyVMT<sup>+/-</sup> male mice were interbred with MKR<sup>+/+</sup> or wild-type (WT) female mice to generate cohorts of WT, MKR<sup>+/+</sup>, PyVMT<sup>+/-</sup>, and PyVMT<sup>+/-</sup>/MKR<sup>+/+</sup> female mice. Only virgin female mice were analyzed in this study. Body weights were recorded weekly until termination of the study. To monitor tumor growth in mammary glands, each of the 10 mammary glands was examined by finger palpation once a week starting at 6 wk of age. Tumor volume was measured by calipers in a three-coordinate system and calculated using the following formula:  $4/3 \times \pi \times (\text{width}/2) \times (\text{length}/2) \times (\text{depth}/2)$ , which represents the three-dimensional volume of an ellipse. Animals were sacrificed when one tumor dimension reached 2 cm. Before euthanasia, blood was collected from the retro-orbital sinus. After euthanasia, all mammary tumors were carefully excised and weighed. Portions of the tumors were either snap frozen in liquid nitrogen or stored in formalin for further studies.

**Syngeneic orthotopic tumor models.** Met-1 and MCNeuA mouse carcinoma cells derived from MMTV-PyVMT/FVB-N and MMTV-Neu/FVB-N transgenic animals were used for orthotopic inoculation into the mammary fat pads of 8-wk-old MKR<sup>+/+</sup> and WT female mice. Cells were allowed to grow until confluence, detached by nonenzymatic cell dissociation solution, and either 500,000 Met-1 cells or 1,000,000 MCNeuA cells, resuspended in 100  $\mu$ L of sterile PBS, were injected into the left inguinal (#4) mammary fat pad using a 30-gauge needle. Monitoring of tumor growth and processing of blood and tissues were performed as described above.

**Densitometric analysis.** Densitometric analyses of immunoblots were performed using MacBAS V2.52 software.

**Statistical analysis.** Results are expressed as the mean  $\pm$  SE. Statistical analyses were calculated using the Student's *t* test or, when appropriate, two-factor ANOVA followed by Holm-Sidak post hoc test.

Additional experimental protocols have been described in Supplementary Data.

## Results

**Metabolic abnormalities in MKR<sup>+/+</sup> mice.** In the present work, the transgenic MKR mouse model of T2D was used (13). In this model, the transgene encoding human IGF-IR has a point mutation in the ATP-binding domain and is driven by the muscle creatine kinase promoter, resulting in inactivation of IR and IGF-IR exclusively in skeletal muscle. Male MKR<sup>+/+</sup> mice develop severe diabetes (13); female MKR<sup>+/+</sup> mice were not extensively studied as they did not exhibit marked hyperglycemia. Herein, we show that female MKR<sup>+/+</sup> mice develop a mild diabetic phenotype, which recapitulates early stages of T2D (prediabetes) in humans. These gender-specific differences may be attributed to estrogens, which exert a protective effect on pancreatic  $\beta$  cells (14). Marked hyperinsulinemia and severe insulin resistance (shown by insulin tolerance test) are the major metabolic abnormalities detected in MKR<sup>+/+</sup> female mice (Fig. 1A). In addition, MKR<sup>+/+</sup> females display a mild dysglycemia shown by slightly elevated blood glucose levels (by  $\sim$ 20%) and impaired glucose tolerance (Fig. 1B). Importantly, MKR<sup>+/+</sup> females are not obese; in fact, they have moderately reduced total body weight and body adiposity compared with WT controls (Fig. 1C). In addition, MKR<sup>+/+</sup> female mice do not show exacerbated inflammatory response observed in obesity and lipotrophic diabetes (data not shown).

**Effect of T2D on mammary gland development.** Little is known about the role of insulin in mammary gland development, but it is well established that IGF-I, which is structurally related to insulin, regulates certain stages of mammary gland development (15). Because MKR<sup>+/+</sup> females develop hyperinsulinemia at a prepubertal age (3 weeks), we assessed whether elevated insulin levels could affect mammary gland development.

At the onset of puberty, the immature mammary gland undergoes rapid growth and differentiation mediated by terminal end buds (TEB) that cause ductal elongation and branching (16). Prepubertal mammary glands in 3-week-old MKR<sup>+/+</sup> mice have increased number and size of TEBs compared with WT glands (Fig. 2A). Additionally, late virgin glands obtained from 15-week-old MKR<sup>+/+</sup> females show increased number of lateral buds and enhanced side branching (Fig. 2B).

The biological effects of insulin and IGFs are mediated by the structurally related IR and IGF-IR. Both the IR and the IGF-IR bind insulin and IGFs, although each receptor binds its cognate ligand with much higher affinity. The two receptors transduce an intracellular signal primarily through the PI3K pathway and the mitogen-activated protein kinase (MAPK) pathway (17).

Given the different properties of each receptor, we wished to determine which receptor and signaling pathway(s) were responsible for the promoting effect of T2D on mammary gland development. For this purpose, mammary epithelial cells (MEC) were isolated from late virgin glands of 15-week-old WT and MKR<sup>+/+</sup> female mice, and extracted cellular proteins were subjected to quantitative analysis of IR and IGF-IR levels by ELISA. Our data show that the level of IR

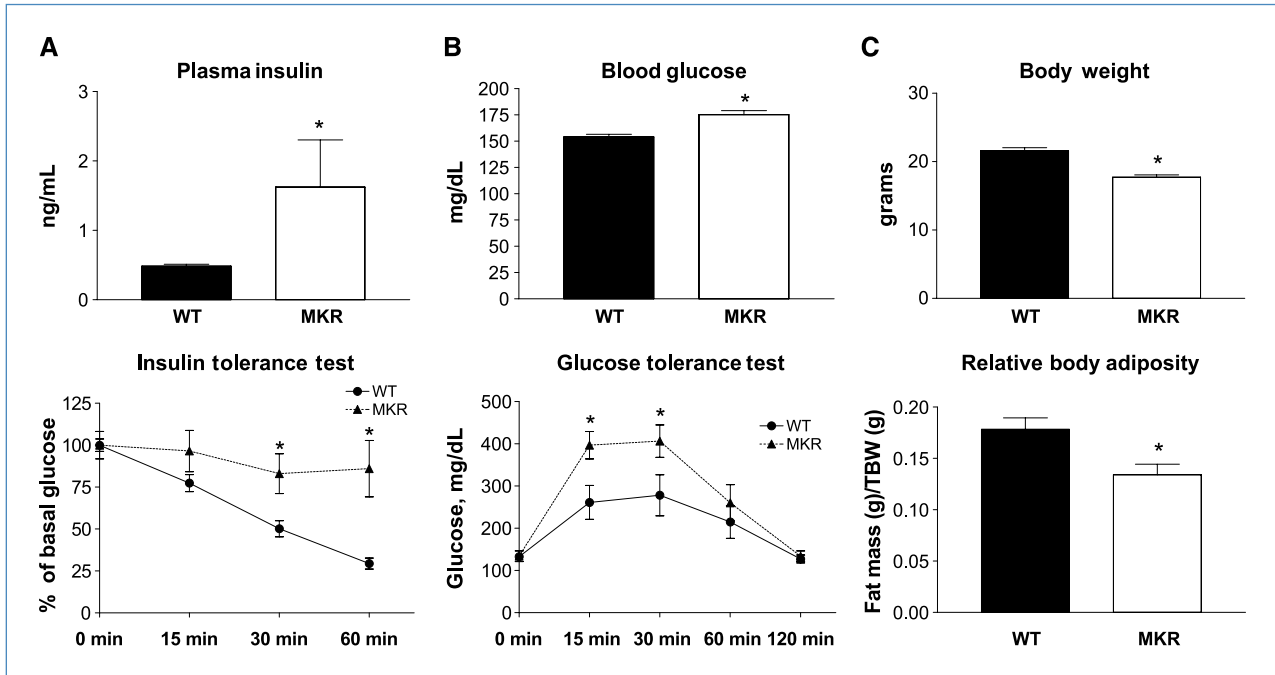


**Figure 1.** Metabolic abnormalities in MKR<sup>+/+</sup> female mice. *A, top*, plasma insulin levels in 8-week-old WT (black column) and MKR<sup>+/+</sup> (white column) mice ( $n = 7$ ); *bottom*, insulin tolerance test was performed on fasted 12-week-old WT (●) and MKR<sup>+/+</sup> (▲) mice ( $n = 5$ ) after i.p. injection of insulin (0.75 units/kg). Blood samples were obtained from the tail vein, and glucose concentrations were determined at the indicated time points. *B, top*, blood glucose in 12-week-old WT (black column) and MKR<sup>+/+</sup> (white column) mice ( $n = 15$ ); *bottom*, glucose tolerance test was performed on fasted 10-week-old WT (●) and MKR<sup>+/+</sup> (▲) mice ( $n = 5$ ) after i.p. injection of glucose (2 g/kg). Blood samples were obtained from the tail vein, and glucose concentrations were determined at the indicated time points. *C*, total body weight (TBW) and total body adiposity in 10- to 12-week-old WT (black columns) and MKR<sup>+/+</sup> (white columns) mice ( $n = 6$ ). Columns and points, mean; bars, SE. Statistically significant difference between WT and MKR groups is indicated. \*,  $P < 0.05$ , Student's  $t$  test.

in mammary epithelium of MKR<sup>+/+</sup> mice is 3-fold higher than in WT mice (Fig. 2C). IGF-IR levels are not significantly different in WT and MKR groups (data not shown). In contrast to MECs, total IR levels in the whole breast tissue are not different in WT and MKR<sup>+/+</sup> mice (Fig. 2D), suggesting that the IR is upregulated in mammary epithelium but not in the stroma of MKR<sup>+/+</sup> mice. However, whole breast tissue obtained from MKR<sup>+/+</sup> mice reveals markedly elevated IR/IGF-IR and Akt phosphorylation (7- and 4-fold, respectively), whereas the level of extracellular signal-regulated kinase 1/2 (ERK1/2) phosphorylation does not differ significantly between the two groups (Fig. 2D and E). These results suggest that in whole mammary tissue hyperinsulinemia results in the activation of IR and/or IGF-IR and a further signal transduction primarily through the PI3K pathway.

Sex steroids and IGF-I are key regulators of mammary gland development (15). Insulin regulates the levels of total and free IGF-I and estrogens by stimulating *igf1* gene expression and steroidogenesis (18, 19) and suppressing IGF-binding protein (IGFBP)-1, IGFBP-2, and sex hormone-binding globulin expression and secretion (7). In MKR<sup>+/+</sup> females, circulating levels of IGF-I and estradiol are not elevated. However, serum IGFBP-1 and IGFBP-2 levels in MKR<sup>+/+</sup> mice are 30% lower than in WT controls (Supplementary Fig. S1). Therefore, it is conceivable that accelerated mammary gland development in MKR<sup>+/+</sup> mice is also mediated by local IGFs,

whose bioavailability is increased due to decreased levels of IGFBP-1 and IGFBP-2.

**Effect of T2D on mammary carcinogenesis.** To study the effect of T2D on breast cancer development, we used several models of mouse mammary carcinogenesis, including the double transgenic PyVmt/MKR model and the syngeneic Met-1 and MCNeuA orthotopic models. In the PyVmt model, the transgene encodes a powerful oncogene (PyVmt) and is controlled by the MMTV promoter, whereby the oncogene is primarily expressed in mammary epithelium (12). PyVmt-induced mammary carcinogenesis shows numerous genetic, morphologic, and pathophysiologic similarities with human breast cancer. A stage-related loss of estrogen receptors (ER) as well as ErbB2/Neu and cyclin D1 overexpression seen in human breast cancer are reproduced in this model (20).

To study the effect of T2D on tumor development in the MMTV-PyVmt model, cohorts of PyVmt<sup>+/+</sup> and PyVmt<sup>+/+</sup>/MKR<sup>+/+</sup> female mice were generated. A unique feature of tumor development in the PyVmt model is that at early stages of tumorigenesis (6 weeks), the primary tumor develops as a single focus on the ducts connected to the nipple (20). In PyVmt<sup>+/+</sup>/MKR<sup>+/+</sup> animals, however, the tumors have a diffuse pattern, with a primary focus and multiple secondary foci (Fig. 3A). Moreover, compared with PyVmt<sup>+/+</sup> mice, PyVmt<sup>+/+</sup>/MKR<sup>+/+</sup> mice show marked ductal hyperplasia

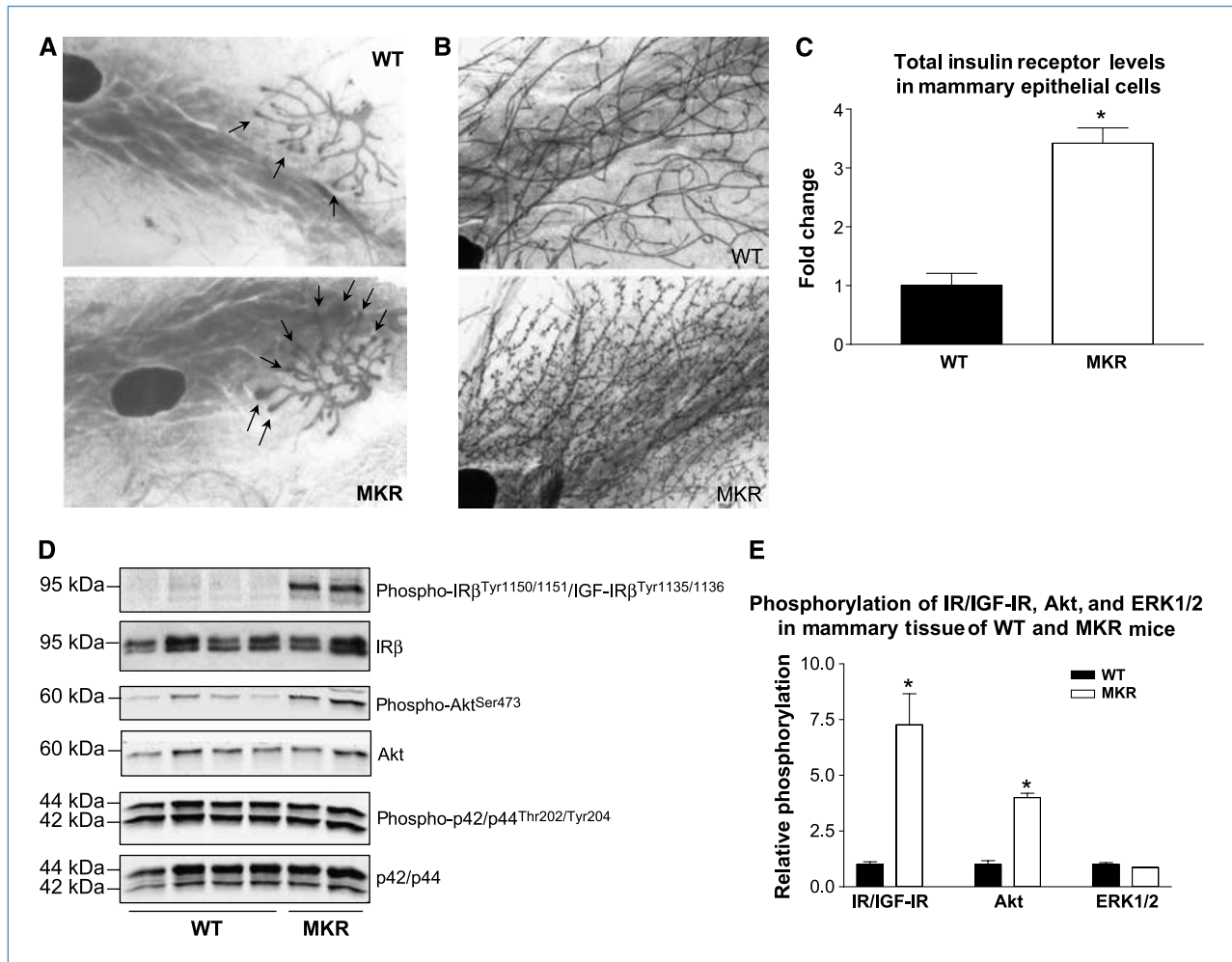


**Figure 2.** Effect of T2D on normal mammary gland development. Whole-mount analysis of prepubertal (3 wk; A) and late virgin (15 wk; B) mammary glands obtained from WT and MKR<sup>+/+</sup> female mice. Arrows, TEBs. Original magnification,  $\times 16$ . Representative image of seven mice. C, total IR levels in MECs isolated from 15-week-old WT and MKR<sup>+/+</sup> virgin female mice ( $n = 3$ ) were measured by ELISA. Relative levels of total IR receptor levels are expressed as fold change compared with WT. Statistically significant difference is indicated. \*,  $P < 0.05$ , Student's  $t$  test. D, proteins (50  $\mu$ g) extracted from mammary tissue of virgin 7-week-old WT and MKR<sup>+/+</sup> mice were size fractionated by SDS-PAGE and immunoblotted with anti-phospho-IR $\beta^{\text{Tyr}1150/1151}$ /IGF-IR $\beta^{\text{Tyr}1135/1136}$ , anti-phospho-Akt<sup>S473</sup>, and anti-phospho-p42/p44<sup>T202/Y204</sup> antibodies. Total level of proteins was shown by immunoblotting with antibodies directed against total IR $\beta$ , Akt, and p42/p44. At least four animals per group were analyzed, and the representative blots are included. E, the results of densitometric analyses of IR/IGF-IR, Akt, and ERK1/2 phosphorylation are presented as a fold change compared with WT mammary tissue. Statistically significant difference is indicated. \*,  $P < 0.05$ , Student's  $t$  test.

and increased number of ducts in intact mammary tissue (Fig. 3B).

To explore whether hyperinsulinemia underlies the tumor-promoting effects of T2D, we studied IR and IGF-IR phosphorylation as well as intracellular signal transduction in PyVmT<sup>+/-</sup> and PyVmT<sup>+/-</sup>/MKR<sup>+/+</sup> mammary tissue. Mammary tissue from PyVmT<sup>+/-</sup>/MKR<sup>+/+</sup> mice displays markedly higher phosphorylation of the IR/IGF-IR and Akt, whereas ERK1/2 phosphorylation is unaffected (Fig. 3C and D). Moreover, because Western blot analysis with phospho-IR/IGF-IR antibody does not allow us to discriminate between the phosphorylated forms of the IR and IGF-IR, we used immunoprecipitation of each receptor followed by immunodetection with the respective phosphospecific anti-

bodies. The IR and, to lesser extent, the IGF-IR are hyperphosphorylated in mammary tumor tissue extracted from diabetic mice (1.7- and 1.4-fold increase, respectively; Supplementary Fig. S2). Our Western blot data also indicate that ER $\alpha$  loss is not accelerated in this model (Supplementary Fig. S3).

To study the effect of T2D on breast cancer progression, we also used the syngeneic Met-1 and MCNeuA orthotopic models. These models allow us to focus on the effect of T2D on growth of fully transformed MECs, whereas in the double transgenic mice the entire tumorigenic process, including preneoplastic stages, is affected by the diabetic milieu. The syngeneic models enable us to study the effect of T2D at specific time points, and, in contrast to the



commonly used xenograft tumor models, they allow us to observe tumorigenesis in the setting of intact immunity.

ER $\alpha$ -negative Met-1 and MCNeuA cell lines were originally derived from PyVmT- and Neu-induced mammary tu-

mors, respectively (21, 22). *Neu* is a rodent analogue of the human *ERBB2* gene, which is amplified and overexpressed in 30% of human breast carcinomas (23). In contrast to Met-1 cells, which show a mesenchymal phenotype and a high

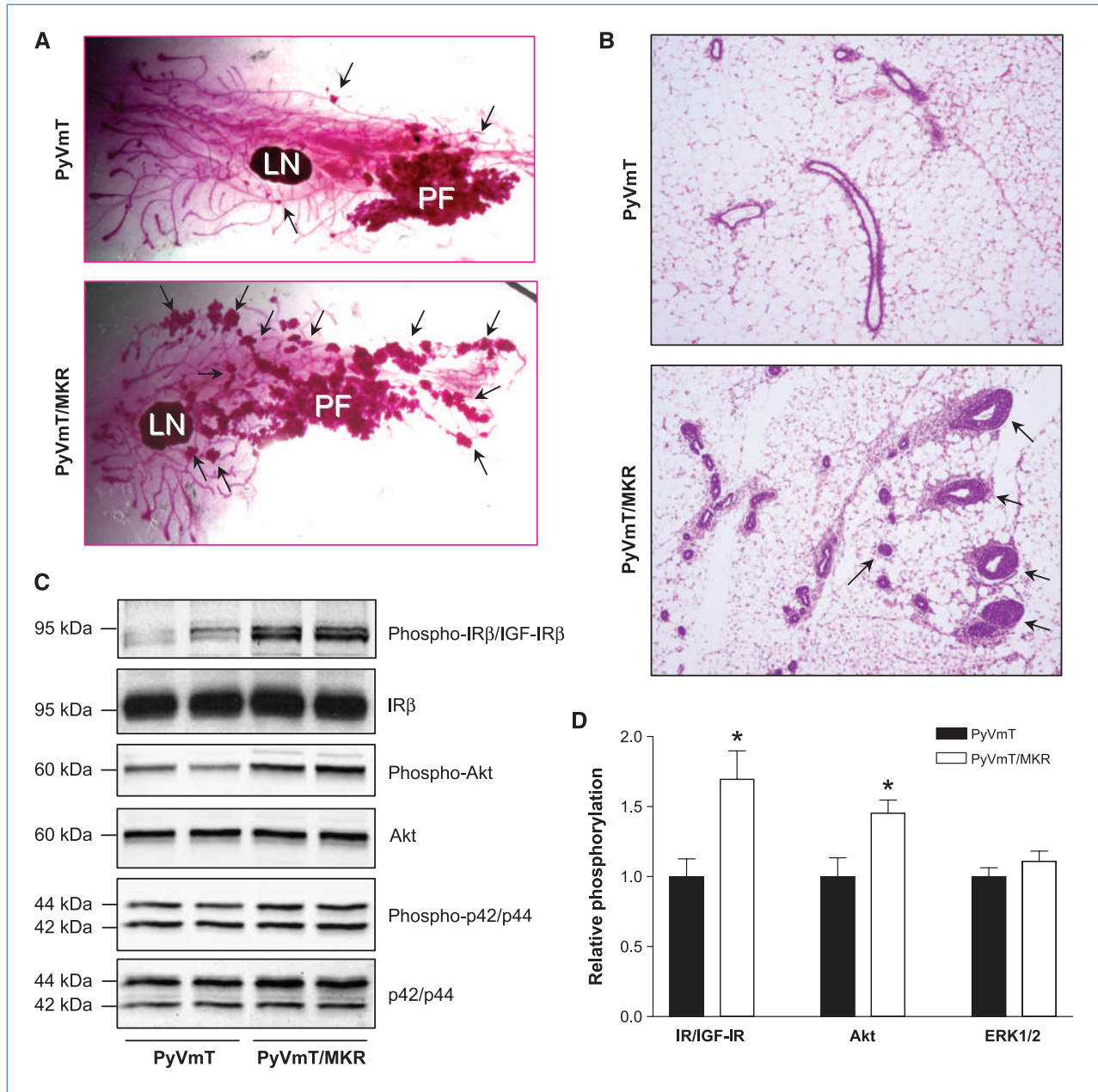


**Figure 3.** Effect of T2D on PyVmT-induced mammary hyperplasia. Whole-mount (A) and histologic analysis (B) of mammary glands obtained from virgin 6-week-old PyVmT<sup>+/-</sup> and PyVmT<sup>+/-</sup>/MKR<sup>+/+</sup> female mice. Arrows, secondary hyperplastic foci (A) and ductal hyperplasia (B). At least seven animals per group were analyzed, and the representative images are included. LN, lymph node; PF, primary tumor focus. Original magnification,  $\times 4$  (A) and  $\times 100$  (B). C, proteins (50  $\mu$ g) extracted from mammary tissue of virgin 7-week-old PyVmT<sup>+/-</sup> and PyVmT<sup>+/-</sup>/MKR<sup>+/+</sup> mice were size fractionated by SDS-PAGE and immunoblotted with anti-phospho-IR $\beta$ <sup>Y1150/S51</sup>/IGF-IR $\beta$ <sup>Y1135/36</sup>, anti-phospho-Akt<sup>S473</sup>, and anti-phospho-p42/p44<sup>T202/Y204</sup> antibodies. Total level of proteins was shown by immunoblotting with antibodies directed against total IR $\beta$ , Akt, and p42/p44. At least seven animals per group were analyzed, and the representative blots are included. D, the results of densitometric analysis of IR/IGF-IR, Akt, and ERK1/2 phosphorylation in PyVmT<sup>+/-</sup> and PyVmT<sup>+/-</sup>/MKR<sup>+/+</sup> mammary tissue are presented as a fold change compared with PyVmT<sup>+/-</sup> mammary tissue. Statistically significant difference is indicated. \*,  $P < 0.05$ , Student's *t* test.

proliferation rate, MCNeuA cells show an epithelial phenotype and a low proliferation rate (data not shown). Both cell types are tumorigenic when implanted back into syngeneic FVB/N mice. We inoculated 500,000 Met-1 cells and 1,000,000 MCNeuA cells into the inguinal mammary fat pad (#4) of MKR<sup>+/+</sup> and WT females and monitored tumor growth. Tumor growth is markedly increased (approximately 3- to 5-fold) in MKR<sup>+/+</sup> mice orthotopically inoculated with either Met-1 or MCNeuA cells (Figs. 4A and B and 5A and B). Furthermore, Met-1 and MCNeuA tumor tissues extracted from MKR<sup>+/+</sup> mice display significantly elevated levels of IR/IGF-IR phosphorylation compared with WT controls (Fig. 4C and D and 5C and D). In addition, MKR<sup>+/+</sup> mice also show a markedly enhanced phosphorylation of Akt and a

moderate increase in ERK1/2 phosphorylation in both tumor models (Fig. 4C and D and 5C and D). Taken together, data from the transgenic and orthotopic models suggest that hyperinsulinemia, acting directly through the IR and/or indirectly through the IGF-IR, further transduces an intracellular signal primarily through the PI3K pathway and augments tumor development in MKR<sup>+/+</sup> mice.

**Effect of pharmacologic IR/IGF-IR blockade on the tumor-promoting activity of T2D.** To corroborate that hyperinsulinemia, IR/IGF-IR activation, and accelerated tumor growth in diabetic animals are mechanistically linked, we used a small-molecule tyrosine kinase inhibitor, BMS-536924 (24). This compound blocks the ATP-binding cleft, which shows 100% sequence identity in the IR and the

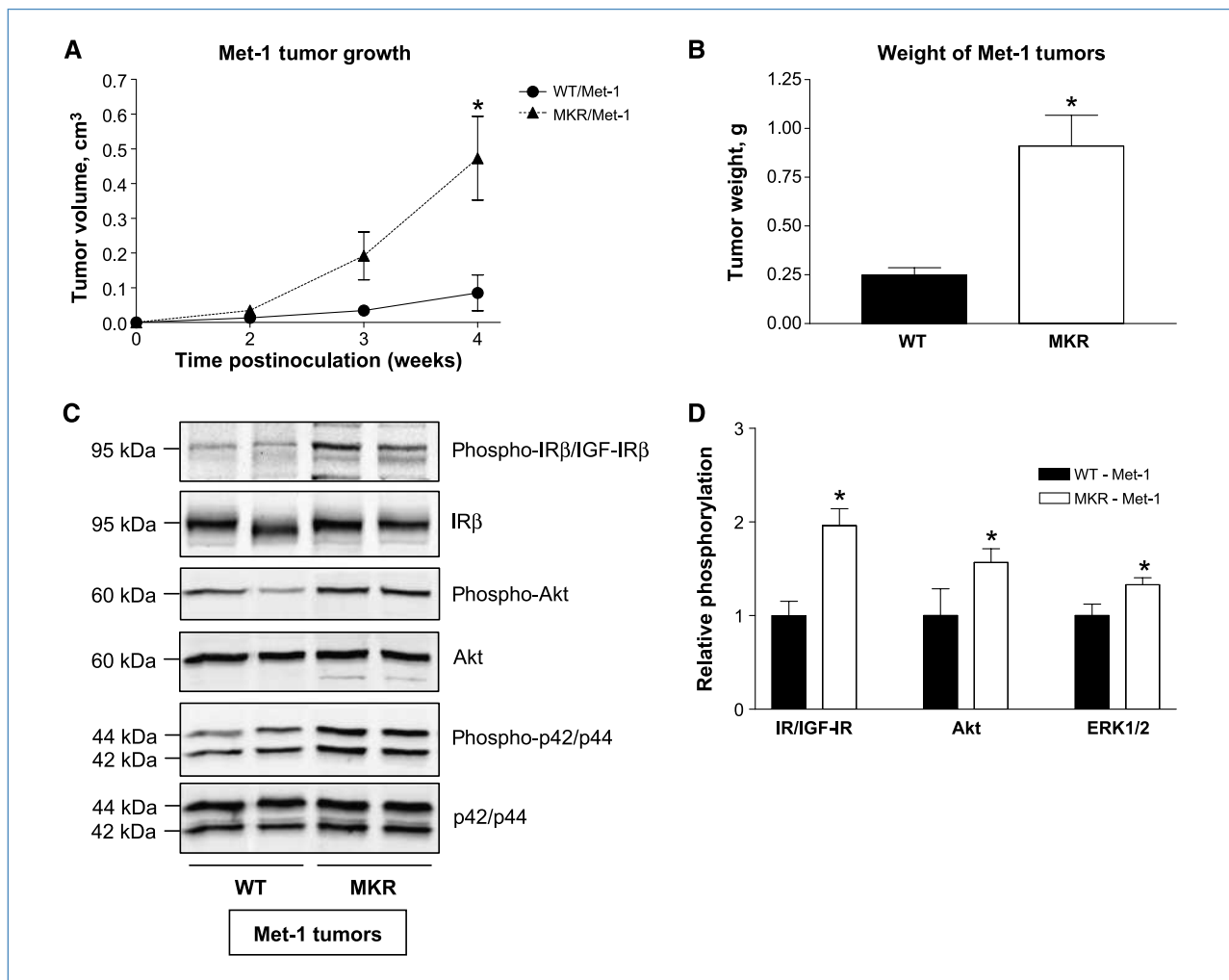


**Figure 4.** Growth (A) and terminal weight (B) of Met-1 tumors obtained from WT and MKR<sup>+/+</sup> female mice (seven animals per group; 4 wk after orthotopic inoculation of 500,000 Met-1 cells). This study was replicated thrice; the representative graphs are presented. Statistically significant difference is indicated. \*,  $P < 0.05$ , Student's  $t$  test. C, proteins (50  $\mu$ g) extracted from Met-1 tumor tissues were size fractionated by SDS-PAGE and immunoblotted with anti-phospho-IR $\beta$ <sup>Y1150/S1</sup>/IGF-IR $\beta$ <sup>Y1135/S6</sup>, anti-phospho-Akt<sup>S473</sup>, and anti-phospho-p42/p44<sup>T202/Y204</sup> antibodies. Total level of proteins was shown by immunoblotting with antibodies directed against total IR $\beta$ , Akt, and p42/p44. Five animals per group were analyzed, and the representative blots are included. D, the results of densitometric analysis of IR/IGF-IR, Akt, and ERK1/2 phosphorylation in Met-1 tumor tissue are presented as a fold change compared with WT tumor tissue. Statistically significant difference is indicated. \*,  $P < 0.05$ , Student's  $t$  test.

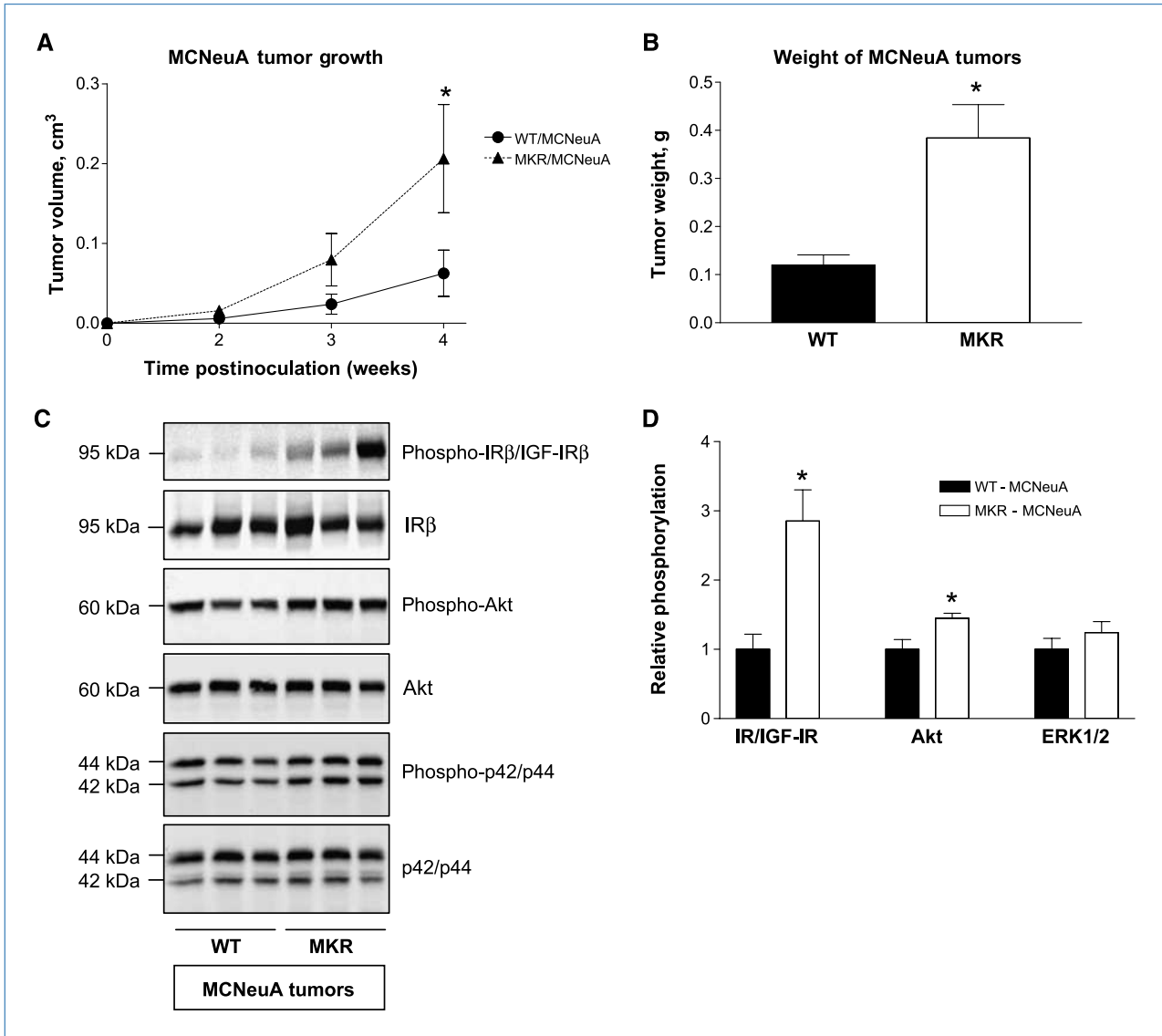


**Figure 5.** Growth (A) and terminal weight (B) of MCNeuA tumors obtained from WT and MKR<sup>+/+</sup> female mice (four to seven animals per group; 4 wk after orthotopic inoculation of 1,000,000 MCNeuA cells). This study was replicated thrice; the representative graphs are presented. Statistically significant difference is indicated. \*,  $P < 0.05$ , Student's  $t$  test. C, proteins (50  $\mu$ g) extracted from MCNeuA tumor tissues were size fractionated by SDS-PAGE and immunoblotted with anti-phospho-IR $\beta$ <sup>Y1150/S1</sup>/IGF-IR $\beta$ <sup>Y1135/36</sup>, anti-phospho-Akt<sup>S473</sup>, and anti-phospho-p42/p44<sup>T202/Y204</sup> antibodies. Total level of proteins was shown by immunoblotting with antibodies directed against total IR $\beta$ , Akt, and p42/p44. Three to five animals per group were analyzed, and the representative blots are included. D, the results of densitometric analysis of IR/IGF-IR, Akt, and ERK1/2 phosphorylation in MCNeuA orthograft tumor tissue are presented as a fold change compared with WT tumor tissue. Statistically significant difference is indicated. \*,  $P < 0.05$ , Student's  $t$  test.

IGF-IR. This mechanism of tyrosine kinase inhibition makes BMS-536924 a fully nonselective dual-receptor inhibitor. In Met-1 cells, insulin-induced and IGF-I-induced signaling is markedly suppressed in the presence of BMS-536924 both *in vitro* and *in vivo* (Supplementary Figs. S4 and S5). To study the effect of IR and IGF-IR blockade *in vivo*, WT and MKR<sup>+/+</sup> female mice were subjected to orthotopic inoculation of Met-1 cells as described above. Three weeks after cell inoculation, WT and MKR<sup>+/+</sup> mice were treated with BMS-536924 or respective vehicle (80% polyethylene glycol, 20%

water; 100 mg/kg/d, orally by gavage) for 2 weeks. Tumor volume and metabolic parameters were determined weekly. Our results indicate that BMS-536924 does not affect tumor growth or carbohydrate metabolism in WT mice (Fig. 6). In contrast, in MKR<sup>+/+</sup> mice, treatment with BMS-536924 results in a moderate increase in blood glucose levels (Fig. 6A), an impairment of glucose tolerance (data not shown), and a marked elevation of plasma insulin levels (Fig. 6B). However, despite exacerbated hyperinsulinemia, tumor growth is significantly attenuated in MKR<sup>+/+</sup> mice treated

with BMS-536924 (Fig. 6C and D), suggesting that the IR and/or the IGF-IR are the predominant mediators of the tumor-promoting activity of T2D in general and hyperinsulinemia in particular.

## Discussion

Numerous epidemiologic studies suggest that obesity and T2D significantly affect the development of many cancers, including breast cancer. However, a positive correlation between obesity, T2D, and breast cancer is mainly observed among postmenopausal women (1, 3–5). In turn, animal studies show that diet-induced metabolic derangements promote mammary carcinogenesis irrespective of ovarian function, but they do not explain the molecular basis of this association (11). An attempt to uncouple the tumor-promot-

ing effect of body adiposity from diabetes was done by using the transgenic A-ZIP/F-1 mouse model of lipoatrophic form of T2D (25). Although these data clearly suggest a direct role of the diabetic milieu in tumor development, the study does not dissect a pathophysiologic mechanism underlying this phenomenon.

In the current work, we used a unique transgenic MKR model of T2D, in which severe insulin resistance and hyperinsulinemia are observed in the setting of moderately reduced body adiposity and mild dysglycemia. MKR female mice show accelerated mammary gland development and breast cancer progression independent of obesity and inflammation. In addition, we show that the signaling axis, including insulin, IR/IGF-IR, and the PI3K/Akt pathway, is the major pathophysiologic mechanism mediating this effect.

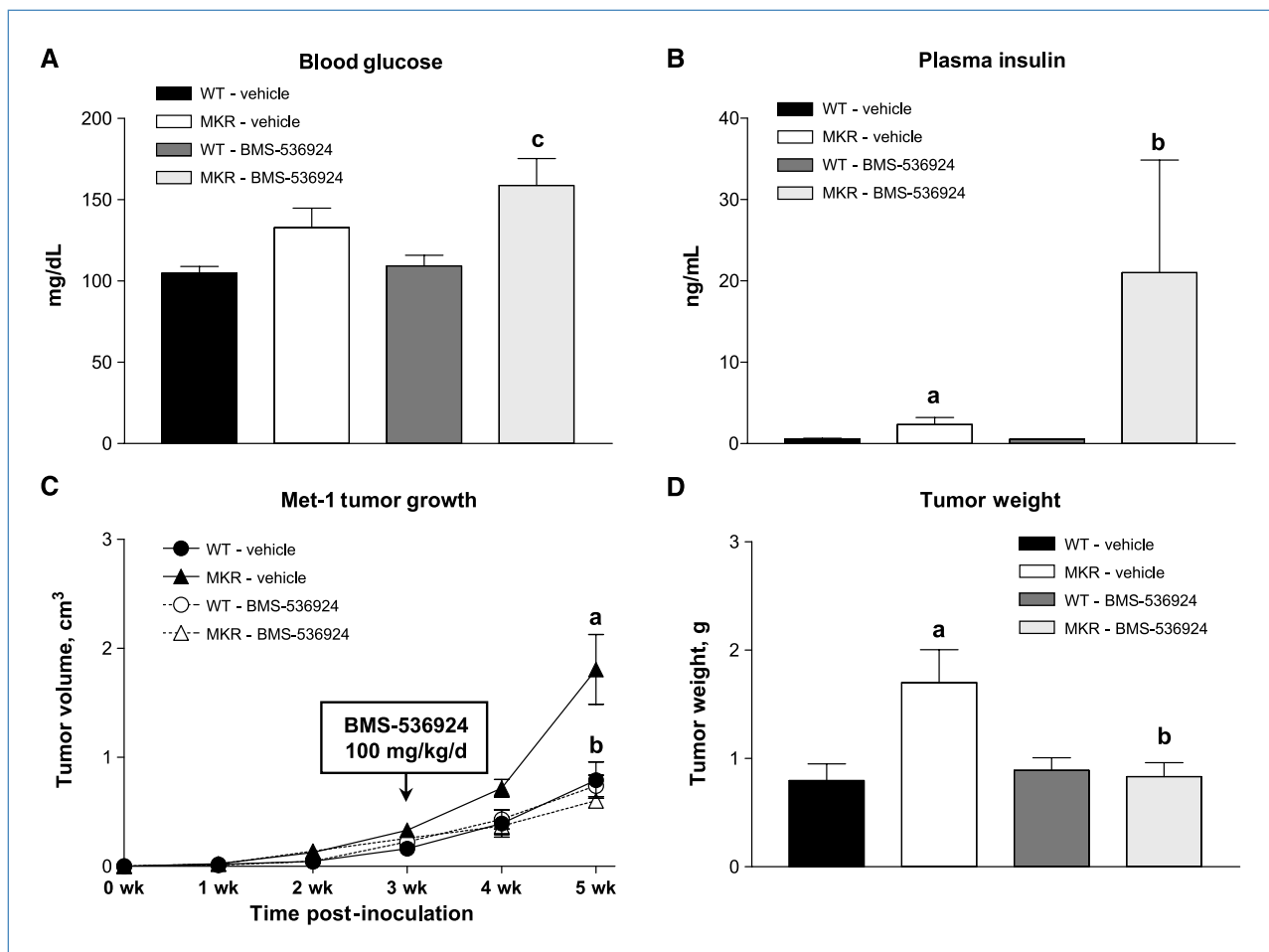


**Figure 6.** Effect of pharmacologic IR/IGF-IR blockade on Met-1 tumor growth and carbohydrate metabolism in MKR<sup>+/+</sup> female mice. Eight-week-old WT and MKR<sup>+/+</sup> female mice ( $n = 5$ ) were subjected to orthotopic inoculation of 500,000 Met-1 cells. Three weeks after tumor inoculation, small-molecule IR/IGF-IR tyrosine kinase inhibitor BMS-536924 (100 mg/kg/d, orally by gavage) or the respective vehicle (80% polyethylene glycol, 20% water) was applied for the next 14 d. Blood glucose (A) and plasma insulin levels (B) in vehicle-treated or BMS-536924-treated WT and MKR<sup>+/+</sup> female mice at the end of the study. Growth (C) and terminal weight (D) of Met-1 tumors obtained from WT and MKR<sup>+/+</sup> female mice treated with vehicle or BMS-536924. Statistically significant difference ( $P < 0.05$ , two-factor ANOVA followed by Holm-Sidak post hoc test) is indicated: (a) WT-vehicle versus MKR-vehicle, (b) MKR-vehicle versus MKR-BMS-536924, and (c) WT-BMS-536924 versus MKR-BMS-536924.



*In vivo*, endogenous insulin may have a tumor-promoting activity, which has been underestimated for a long time. Reduction of insulin levels in animals with chemically induced type 1 diabetes (T1D) resulting from the destruction of pancreatic  $\beta$  cells suppresses tumor growth, whereas insulin administration abrogates this effect (26–30). Furthermore, intraportal transplantation of pancreatic islets into rats with T1D results in the development of an insulin-enriched microenvironment promoting hepatocellular transformation (31). These studies, which used experimental models of T1D, thus link insulin and cancer mechanistically and indicate that insulin plays a role of both tumor promoter and tumor initiator. In line with these data, our results strongly support the tumor-promoting effect of elevated circulating insulin levels in T2D in the setting of severe insulin resistance and normal ovarian function. These data are also in accordance with epidemiologic studies showing a positive correlation between circulating insulin levels and breast cancer risk and mortality (32).

The tumor-promoting activity of insulin can be mediated by direct and indirect mechanisms. Insulin is known to transduce the intracellular signal through its cognate receptor. Indeed, the results of our study show enhanced IR phosphorylation in mammary and tumor tissue extracted from diabetic mice. Our data, however, also show an increase in IGF-IR phosphorylation, suggesting that the tumor-promoting activity of hyperinsulinemia can also be mediated, at least in part, by the IGF-IR. It is well known that at higher concentrations, insulin stimulates the IGF-IR (17, 33). In Met-1 cells, which were used in the current work, IGF-IR activation is observed in response to supraphysiologic concentrations of insulin ( $\geq 50$  nmol/L; physiologic range, 1–10 nmol/L).<sup>6</sup> Therefore, it is plausible that elevated circulating insulin levels may also result in IGF-IR activation *in vivo*. In addition, in certain cell types, insulin activates the IGF-IR at physiologic concentrations (33). Moreover, some cells, including human breast cancer cells, express an atypical IGF-IR, which binds both IGF-I and insulin with high affinity (34). These data further support our hypothesis that the tumor-promoting activity of hyperinsulinemia can be associated with the IGF-IR.

Furthermore, the tumor-promoting activity of hyperinsulinemia can also be mediated by IGFs. Mammary stroma and breast cancer cells are an abundant source of IGFs and IGFBPs (35). Insulin inhibits IGFBP-1 and IGFBP-2 expression (7) and thus increases the bioavailability of IGFs. Our results show a 30% reduction in IGFBP-1 and IGFBP-2 levels in sera of diabetic mice, suggesting a possible role of this mechanism in the tumor-promoting activity of T2D. Alternatively, the promoting action of hyperinsulinemia on mammary gland development and formation of PyVmT-induced hyperplastic lesions can also be mediated by ER $\alpha$ , which interacts with the IGF-IR/IR at multiple cellular levels (36, 37).

<sup>6</sup> Unpublished data.

We also show that IR levels in mammary epithelium of diabetic mice are elevated. The role of the IR in oncogenic transformation and tumorigenesis has not been extensively studied. It is known that IR overexpression results in cellular transformation (38). A functional IR is essential for the transformation of endothelial cells infected by Kaposi sarcoma-associated herpes virus (39). IR upregulation is also observed in mouse mammary epithelium transformed by *wnt-1*, *neu*, and *ret* (40). In addition, human mammary carcinomas show higher IR levels than normal breast tissue (38). Total IR levels in breast tumor tissue are inversely correlated with a disease-free survival (41, 42). These data strongly suggest that in breast tissue the IR has an important biological and clinical relevance.

IR and IGF-IR transduce their intracellular signal through two principal signaling pathways: the MAPK and the PI3K pathway (17). Our data show that signaling through the PI3K pathway is enhanced in normal mammary gland and breast tumor tissue of diabetic animals, suggesting that this pathway may mediate the effects of hyperinsulinemia on normal and transformed cells. Certain stages of mammary gland development are governed by the PI3K/Akt pathway (43), whereas its deregulation and hyperactivation result in tumor transformation (44–48). Targeting the PI3K/Akt pathway, therefore, may be a promising therapeutic option for breast cancer patients with T2D.

Taken together, our data provide compelling evidence that T2D accelerates mammary gland development and breast cancer progression. We hypothesize that due to hyperinsulinemia and increased IR expression, the mammary epithelium in T2D is more susceptible to mitogenic and survival signals, which accelerate mammary gland development and facilitate tumor formation and progression. Mammary carcinogenesis in T2D represents a two-hit phenomenon, with an oncogene (e.g., PyVmT or Neu) acting as a tumor initiator and hyperinsulinemia acting as a tumor promoter. The present study has an important clinical relevance and significant public health implications. Early detection and therapeutic correction of hyperinsulinemia may help to reduce breast cancer morbidity and mortality. Furthermore, our data provide the rationale for pharmacologic targeting of a specific signaling cascade comprising insulin, the IR/IGF-IR, and the PI3K/Akt pathway in breast cancer patients with T2D.

## Disclosure of Potential Conflicts of Interest

No potential conflicts of interest were disclosed.

## Acknowledgments

We thank W.J. Muller (McGill University, Montreal, Quebec, Canada), S.D. Hurstings (Department of Nutritional Sciences, University of Texas, Austin, TX, and Department of Carcinogenesis, University of Texas M. D. Anderson Cancer Center, Smithville, TX) and N.P. Nunez (Department of Nutritional Sciences, University of Texas, Austin, TX), and M.J. Campbell and J.F. Youngren (University of

California San Francisco, San Francisco, CA) for donating MMTV-PyVmt transgenic mice, Met-1 cells, and MCNeuA cells, respectively.

## Grant Support

National Cancer Institute grant IRO1CA128799-O1A1 and Gerald J. and Dorothy R. Friedman Foundation. D.E. Lann was supported by NIH grant T32 DK007792. Y. Fierz

was funded by Swiss National Science Foundation grant PBB5B-120851, Novartis Foundation and Roche Research Foundation.

The costs of publication of this article were defrayed in part by the payment of page charges. This article must therefore be hereby marked *advertisement* in accordance with 18 U.S.C. Section 1734 solely to indicate this fact.

Received 6/22/09; revised 10/7/09; accepted 11/6/09; published OnlineFirst 1/12/10.

## References

1. Renehan AG, Tyson M, Egger M, Heller RF, Zwahlen M. Body-mass index and incidence of cancer: a systematic review and meta-analysis of prospective observational studies. *Lancet* 2008;371:569–78.
2. Bianchini F, Kaaks R, Vainio H. Overweight, obesity, and cancer risk. *Lancet Oncol* 2002;3:565–74.
3. Calle EE, Rodriguez C, Walker-Thurmond K, Thun MJ. Overweight, obesity, and mortality from cancer in a prospectively studied cohort of U.S. adults. *N Engl J Med* 2003;348:1625–38.
4. Xue F, Michels KB. Diabetes, metabolic syndrome, and breast cancer: a review of the current evidence. *Am J Clin Nutr* 2007;86:s823–35.
5. Barone BB, Yeh HC, Snyder CF, et al. Long-term all-cause mortality in cancer patients with preexisting diabetes mellitus: a systematic review and meta-analysis. *JAMA* 2008;300:2754–64.
6. Rose DP, Komninou D, Stephenson GD. Obesity, adipocytokines, and insulin resistance in breast cancer. *Obes Rev* 2004;5:153–65.
7. Calle EE, Kaaks R. Overweight, obesity and cancer: epidemiological evidence and proposed mechanisms. *Nat Rev Cancer* 2004;4:579–91.
8. Vona-Davis L, Howard-McNatt M, Rose DP. Adiposity, type 2 diabetes and the metabolic syndrome in breast cancer. *Obes Rev* 2007;8:395–408.
9. Larsson SC, Mantzoros CS, Wolk A. Diabetes mellitus and risk of breast cancer: a meta-analysis. *Int J Cancer* 2007;121:856–62.
10. Lann D, LeRoith D. The role of endocrine insulin-like growth factor-I and insulin in breast cancer. *J Mammary Gland Biol Neoplasia* 2008;13:371–9.
11. Novosyadlyy R, Vijayakumar A, Fierz Y, LeRoith D. Animal models of hyperinsulinemia, insulin resistance and cancer. In: Fantus IG, editor. New York: Springer. In press 2009.
12. Guy CT, Cardiff RD, Muller WJ. Induction of mammary tumors by expression of polyomavirus middle T oncogene: a transgenic mouse model for metastatic disease. *Mol Cell Biol* 1992;12:954–61.
13. Fernandez AM, Kim JK, Yakar S, et al. Functional inactivation of the IGF-I and insulin receptors in skeletal muscle causes type 2 diabetes. *Genes Dev* 2001;15:1926–34.
14. Le MC, Chu K, Hu M, et al. Estrogens protect pancreatic  $\beta$ -cells from apoptosis and prevent insulin-deficient diabetes mellitus in mice. *Proc Natl Acad Sci U S A* 2006;103:9232–7.
15. Kleinberg DL, Wood TL, Furth PA, Lee AV. Growth hormone and insulin-like growth factor-I in the transition from normal mammary development to preneoplastic mammary lesions. *Endocr Rev* 2008.
16. Hennighausen L, Robinson GW. Signaling pathways in mammary gland development. *Dev Cell* 2001;1:467–75.
17. LeRoith D, Werner H, Beitner-Johnson D, Roberts CT, Jr. Molecular and cellular aspects of the insulin-like growth factor I receptor. *Endocr Rev* 1995;16:143–63.
18. Boni-Schnetzler M, Schmid C, Meier PJ, Froesch ER. Insulin regulates insulin-like growth factor I mRNA in rat hepatocytes. *Am J Physiol* 1991;260:E846–51.
19. Poretsky L, Cataldo NA, Rosenwaks Z, Giudice LC. The insulin-related ovarian regulatory system in health and disease. *Endocr Rev* 1999;20:535–82.
20. Lin EY, Jones JG, Li P, et al. Progression to malignancy in the polyoma middle T oncoprotein mouse breast cancer model provides a reliable model for human diseases. *Am J Pathol* 2003;163:2113–26.
21. Borowsky AD, Namba R, Young LJ, et al. Syngeneic mouse mammary carcinoma cell lines: two closely related cell lines with divergent metastatic behavior. *Clin Exp Metastasis* 2005;22:47–59.
22. Campbell MJ, Wollish WS, Lobo M, Esserman LJ. Epithelial and fibroblast cell lines derived from a spontaneous mammary carcinoma in a MMTV/neu transgenic mouse. *In Vitro Cell Dev Biol Anim* 2002;38:326–33.
23. Slamon DJ, Clark GM, Wong SG, et al. Human breast cancer: correlation of relapse and survival with amplification of the HER-2/neu oncogene. *Science* 1987;235:177–82.
24. Wittman M, Carboni J, Attar R, et al. Discovery of a (1*H*-benzoimidazol-2-yl)-1*H*-pyridin-2-one (BMS-536924) inhibitor of insulin-like growth factor I receptor kinase with *in vivo* antitumor activity. *J Med Chem* 2005;48:5639–43.
25. Nunez NP, Oh WJ, Rozenberg J, et al. Accelerated tumor formation in a fatless mouse with type 2 diabetes and inflammation. *Cancer Res* 2006;66:5469–76.
26. Heuson JC, Legros N, Heimann R. Influence of insulin administration on growth of the 7,12-dimethylbenz(a)anthracene-induced mammary carcinoma in intact, oophorectomized, and hypophysectomized rats. *Cancer Res* 1972;32:233–8.
27. Heuson JC, Legros N. Influence of insulin deprivation on growth of the 7,12-dimethylbenz(a)anthracene-induced mammary carcinoma in rats subjected to alloxan diabetes and food restriction. *Cancer Res* 1972;32:226–32.
28. Cohen ND, Hilf R. Influence of insulin on growth and metabolism of 7,12-dimethylbenz(a)anthracene-induced mammary tumors. *Cancer Res* 1974;34:3245–52.
29. Shafie SM, Grantham FH. Role of hormones in the growth and regression of human breast cancer cells (MCF-7) transplanted into athymic nude mice. *J Natl Cancer Inst* 1981;67:51–6.
30. Sharon R, Pillemer G, Ish-Shalom D, et al. Insulin dependence of murine T-cell lymphoma. II. Insulin-deficient diabetic mice and mice fed low-energy diet develop resistance to lymphoma growth. *Int J Cancer* 1993;53:843–9.
31. Dombrowski F, Bannasch P, Pfeifer U. Hepatocellular neoplasms induced by low-number pancreatic islet transplants in streptozotocin diabetic rats. *Am J Pathol* 1997;150:1071–87.
32. Gunter MJ, Hoover DR, Yu H, et al. Insulin, insulin-like growth factor-I, and risk of breast cancer in postmenopausal women. *J Natl Cancer Inst* 2009;101:48–60.
33. Humpert PM, Djuric Z, Zeuge U, et al. Insulin stimulates the clonogenic potential of angiogenic endothelial progenitor cells by IGF-1 receptor-dependent signaling. *Mol Med* 2008;14:301–8.
34. Milazzo G, Yip CC, Maddux BA, Vigneri R, Goldfine ID. High-affinity insulin binding to an atypical insulin-like growth factor-I receptor in human breast cancer cells. *J Clin Invest* 1992;89:899–908.
35. Wood TL, Richert MM, Stull MA, Allar MA. The insulin-like growth factors (IGFs) and IGF binding proteins in postnatal development of murine mammary glands. *J Mammary Gland Biol Neoplasia* 2000;5:31–42.
36. Smith CL. Cross-talk between peptide growth factor and estrogen receptor signaling pathways. *Biol Reprod* 1998;58:627–32.
37. Fagan DH, Yee D. Crosstalk between IGF1R and estrogen receptor signaling in breast cancer. *J Mammary Gland Biol Neoplasia* 2008;13:423–9.

38. Frasca F, Pandini G, Sciacca L, et al. The role of insulin receptors and IGF-I receptors in cancer and other diseases. *Arch Physiol Biochem* 2008;114:23–37.
39. Rose PP, Carroll JM, Carroll PA, et al. The insulin receptor is essential for virus-induced tumorigenesis of Kaposi's sarcoma. *Oncogene* 2007;26:1995–2005.
40. Frittitta L, Cerrato A, Sacco MG, et al. The insulin receptor content is increased in breast cancers initiated by three different oncogenes in transgenic mice. *Breast Cancer Res Treat* 1997;45:141–7.
41. Mathieu MC, Clark GM, Allred DC, Goldfine ID, Vigneri R. Insulin receptor expression and clinical outcome in node-negative breast cancer. *Proc Assoc Am Physicians* 1997;109:565–71.
42. Law JH, Habibi G, Hu K, et al. Phosphorylated insulin-like growth factor-I/insulin receptor is present in all breast cancer subtypes and is related to poor survival. *Cancer Res* 2008;68:10238–46.
43. Boxer RB, Stairs DB, Dugan KD, et al. Isoform-specific requirement for Akt1 in the developmental regulation of cellular metabolism during lactation. *Cell Metab* 2006;4:475–90.
44. Dupont J, Renou JP, Shani M, Hennighausen L, LeRoith D. PTEN overexpression suppresses proliferation and differentiation and enhances apoptosis of the mouse mammary epithelium. *J Clin Invest* 2002;110:815–25.
45. Saal LH, Holm K, Maurer M, et al. PIK3CA mutations correlate with hormone receptors, node metastasis, and ERBB2, and are mutually exclusive with PTEN loss in human breast carcinoma. *Cancer Res* 2005;65:2554–9.
46. Zhao H, Cui Y, Dupont J, et al. Overexpression of the tumor suppressor gene phosphatase and tensin homologue partially inhibits wnt-1-induced mammary tumorigenesis. *Cancer Res* 2005;65:6864–73.
47. Maroulakou IG, Oemler W, Naber SP, Tschlis PN. Akt1 ablation inhibits, whereas Akt2 ablation accelerates, the development of mammary adenocarcinomas in mouse mammary tumor virus (MMTV)-ErbB2/neu and MMTV-polyoma middle T transgenic mice. *Cancer Res* 2007;67:167–77.
48. Ju X, Katiyar S, Wang C, et al. Akt1 governs breast cancer progression *in vivo*. *Proc Natl Acad Sci U S A* 2007;104:7438–43.